

**SOME OBSERVATIONS ON THE FRACTURE CHARACTERISTICS AND FATIGUE
CRACK GROWTH RATES IN A HIGH STRENGTH ALUMINUM ALLOY**

بعض الملاحظات على خصائص الكسر وشروخ الكلال
لسبيكة ألومنيوم عالية المقاومة

BY

M. A. N. Shabara and A. A. Fattah

Department of Industrial Production
Faculty of Engineering - Mansoura University

خلاصة :

نظراً لأهمية تقدير التكامل الإنشائي والتوقع العمري للأجزاء الهندسية فقد نشأ اهتمام متزايد في الآونة الأخيرة بتوصيف عملية التشريح الكلالى ومقاومة الكسر لمختلف المواد الإنشائية . والحراسة الحائلة موجبة لتعيين كيفية اعتماد خصائص الكسر ونمو الشروخ على المعالجة الحرارية السابق إجراؤها على المادة .

وقد وقع الاختيار على سبيكة الألومنيوم عالية المقاومة 7075 لتكون مادة المحث وذلك بعد إجراء المعالجة الحرارية T6 - المكونة من عمليات المعالجة الذوبانية المتبوعة بعليقتي الإطفاء ثم التشيخ الصناعى - والتي ينتج عنها خصائص جيدة لقوة التحمل والمطولية . وقد تم الاحتفاظ بدرجة حرارة التشيخ ثابتة بينما تم تغيير زمن التشيخ بين ساعتين وعشر ساعات، كما استعملت عينات رقيقة ذات الحدس العفرد لتجارب شروخ الكلال وعينات ذات الحدشين الجانبيين لتجارب متانة الكسر .

وتشير نتائج البحث الى أن تغيير زمن التشيخ فى المدى المذكور ينتج عنه تعبير محوس فى متانة الكسر ومعدل نمو الشروخ، حيث تؤدي الزيادة فى زمن التشيخ الى زيادة معدل نمو الشروخ وخفض متانة الكسر . ويمزى ذلك الى التغيرات الحادثة فى المادة نتيجة عملية التشيخ والترسيب مما يؤثر على قوة الدفع المحللة عند رأس الشرخ ؛ وهذه القوة معروفة بتأثيرها بعدة عوامل منها إغلاق الشرخ ولدونة المادة وانحراف الشرخ عن مساره المعتاد .

ABSTRACT- Because of the importance of assessing the structural integrity and life expectancy of engineering components, there has been considerable effort in the last thirty years in the characterization of fatigue cracking and fracture resistance for different structural materials. The present study is directed to the determination of the type of dependence of the fracture resistance and the fatigue crack initiation and propagation behavior on previous heat treatment performed on the material.

High strength aluminum alloy, type 7075, has been selected as the test material. A successful T6 treatment, consisting of solution treatment followed by quenching and an aging period, results generally in good strength and toughness properties. Aging temperature was kept constant while aging time was varied from two to ten hours. Single-edge notched specimens have been used for fatigue crack propagation test; while double-edge notched specimens have been used for fracture toughness tests.

Test results indicate that variation in the aging time for the alloy results in an appreciable variation in its fracture toughness and the rate of crack growth. Longer aging periods lead to higher crack growth rates and lower fracture toughness. The test results may be explained as being due to variations in the local driving force acting at the crack tip. This force is known to be influenced by several factors such as crack closure, cyclic plasticity, and crack deviation from its regular growth direction.

KEYWORDS

Fatigue crack growth, fracture mechanics, fracture toughness, aluminum alloy, precipitation hardening, crack growth gauge.

NOMENCLATURE

A	a constant in the crack growth equation
a	crack length
a ₀	original notch length
b ₀	specimen width
E	modulus of elasticity of material
F	maximum applied load during fracture toughness test
f (a/b)	a function which accounts for crack shape and dimension
J	energy release rate at the onset of fracture
K _e ^c	plane stress fracture toughness
ΔK	range of the stress intensity factor
λ	particle spacing
m	a constant in the crack growth equation
N	number of loading cycles
t	thickness of test specimen
t _a	aging time
G _c	critical strain energy release rate
ϵ_f	normal strain at fracture
ϵ_0	initial normal strain
σ_0	yield strength of the material
$\Delta \sigma$	stress range
δ_c	critical crack opening displacement
r _{pc}	critical plastic zone size

INTRODUCTION

The last few decades have witnessed tremendous developments in the science of fracture mechanics which is primarily concerned with the behaviour of components containing flaws and microcracks. It has provided the designers with invaluable information regarding the effects of mechanical, environmental and micro-structural factors on the fracture characteristics of these components. Such information are used towards the attainment of fracture-safe designs and the assessment of the structural integrity of mechanical components. The fracture mechanics approach is now in a widespread use particularly for safety-critical structures such as in nuclear and aerospace industries.

While the termination of life of a component may be based on some critical flaw size for large scale fracture, as calculated from the material's fracture toughness, it has long been recognized that the total useful life of a cyclically loaded component is dependent upon the rate of growth of flaws from a subcritical size to a critical size. Therefore, an understanding of the fatigue crack growth characteristics of structural materials under appropriate service conditions is also essential for the evaluation of the structure's useful life.

The characteristics of fatigue crack growth is generally dependent on the state of the stress and strain field near the crack tip which is represented by the range of stress intensity factor, ΔK . Such a dependence is generally describable by a sigmoidal curve in a $\log(da/dN)$ versus $\log \Delta K$ coordinate scale, bounded at the extremes by the threshold stress intensity range, ΔK_{th} , and the critical stress intensity range, ΔK_c , as shown in Fig.1. In the intermediate ΔK range, $\log(da/dN)$ is almost linearly related to $\log \Delta K$, as expressed by the semi-empirical relation proposed by Paris and Erdogan [1]

$$da / dN = A (\Delta K)^m \quad \dots (1)$$

Where A and m are termed material constants indicative of the fatigue crack growth in the intermediate range. These constants are generally determined from the best fit to the experimental data as the intercept and the slope of the straight

line portion of the sigmoidal curve. It must be pointed out that one of the principal limitations of Paris equation, Eq.(1), is that a state of small scale yielding is considered to exist at the crack tip. If extensive local plasticity exists at the crack tip, other alternative analyses have been developed to define the state of the stress and strain at the crack tip. The alternative analyses are based on the J-integral and the crack tip opening displacement concepts [2,3]. In all cases, the initiation of cracking and fracture are characterized by the criterion that the quantities K , J , and δ reach some critical values.

The correlation of the fatigue crack propagation with the stress intensity factor range, as explained above, has been well documented for both mild steels and high strength aluminum alloys [4,5]. The majority of the work done in this direction dealt primarily with variations in the type of materials, applied loads, test specimen, and crack geometry. Studies pertaining to the influence of microstructural parameters on the crack initiation and growth have not been extensive. It was with these points in mind that the present study was initiated. The purpose of the study is the determination of the influence of the precipitation heat treatment performed on the aluminum alloy on the fracture toughness and crack initiation and growth behavior of the alloy.

EXPERIMENTAL PROCEDURE

MATERIAL:

High strength Cu-Mg-Zn-aluminum alloy, type 7075, having a chemical composition as shown in Table 1, has been selected as the test material. This type of material is of the precipitation-hardening type and possesses good strength and ductility properties upon successful T6 treatment and is widely used in aerospace applications. Thin specimens having a nominal thickness of 1.270 mm were first solution treated for one hour at 482°C in a salt bath, quenched in iced water, and then artificially aged at a temperature of 177°C for aging times ranging from two to ten hours. All temperatures were maintained reasonably within the specified limits. The nominal mechanical properties of the alloy are shown in Table 2.

Table 1 Chemical Composition of Aluminum Alloy 7075

Cu	Mg	Zn	Cr	Al
1.5 %	2.5 %	5.5 %	0.3 %	90.2 %

Table 2 Mechanical Properties of Aluminum Alloy 7075

0.2% Yield Strength MPa	Ultimate Tensile Strength MPa	%Elongation in 50 mm G. Length
500	750	11

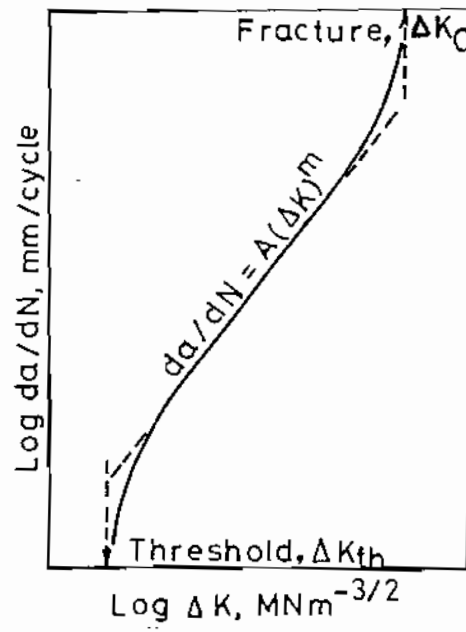


Fig.1 Fatigue Crack Growth Curve

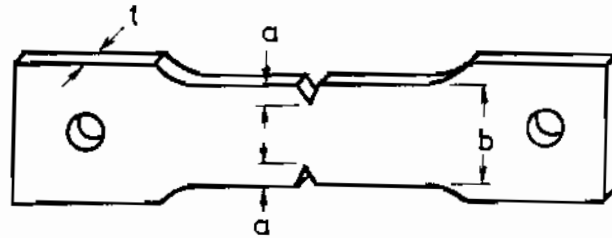


Fig.2 Plane stress fracture toughness specimen

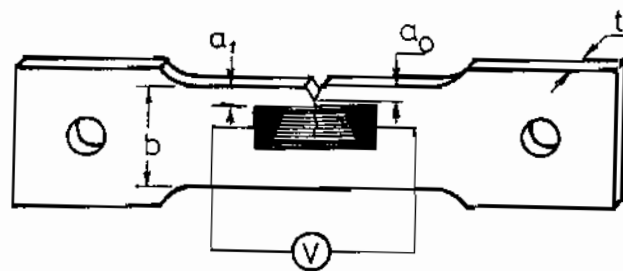


Fig.3. Fatigue Crack Growth Specimen

SPECIMENS:

Plane stress fracture toughness for the alloy were determined using double-edge notched specimens, as shown in Fig.2. On the other hand, single-edge notched specimens, shown in Fig.3, have been used for fatigue crack growth experiments. All tests have been conducted at ambient temperature. Notches have been cut on the milling machine and the notch depths were accurately measured using a travelling microscope. Table 3 shows the dimensions of the specimens tested for fracture toughness and fatigue crack growth. Three specimens have been tested for each aging time in order to obtain meaningful average values for the test parameters.

Table 3 Dimensions of Specimens

Specimen	Ageing Time, hours	a_0 , mm	a_1 , mm	b, mm	t, mm
1	2	4.445	4.700	25.4	1.143
2	2	4.826	5.080	25.4	1.143
3	2	4.616	4.720	25.4	1.143
4	5	4.554	4.610	25.4	1.143
5	5	4.750	4.941	25.4	1.143
6	5	4.855	5.055	25.4	1.143
7	10	4.572	4.572	25.4	1.143
8	10	4.700	4.800	25.4	1.143
9	10	4.652	4.775	25.4	1.143

(I) Fracture Toughness Tests

Double-edge notched fracture toughness specimens were pulled to a complete separation on a tensile testing machine at a load range of 26.8 kN and a head speed of 6.35 mm/min. The fracture toughness were calculated from the maximum tensile load at which each specimen had failed.

(II) Fatigue Crack Propagation Tests

Fatigue crack growth testing was conducted on the JJ-Lloyd tensile machine Model T22K with cycler. The machine was preset at a mean load of 2 KN and a load range of 11/2 KN. Crack length was determined periodically as a function of the number of loading cycles using fatigue crack propagation gauges mounted on each specimen, as shown in Fig.3. Each gauge consisted of a number of five strands which break one after the other as the crack advances through the width of the specimen. This gives rise to a sudden change in the reading of the voltage passing through the electronic gauge. The distance travelled by the crack was accurately measured using this method since each gauge had a known width which contained twenty equidistant fine strands. The jump in the voltage was also detected on an X-Y recorder. The experiment was stopped immediately after the breakage of the last strand in the gauge.

TEST RESULTS

The plane stress fracture toughness were calculated from the fracture load using the formula [6]

$$K_C = (F \sqrt{a}/tb) [1.98 + 0.36(2a/b) - 2.12(2a/b)^2 + 3.42(2a/b)^3] \quad \dots (2)$$

It must be noted that Equation (2) assumes that the material behaves in a linear manner up to fracture and, therefore, it does not take into account the effect of plasticity. In order to account for plasticity effects, the toughness should be calculated using a modified crack length which includes a plastic zone size, r_p , calculated from the formula [7]:

$$r_p = (1/2\pi) (K_c/\sigma_0)^2 \quad \dots (3)$$

Other fracture characteristics such as the critical energy release rate, G_c , the critical crack opening displacement, δ_c , and the critical plastic zone size, r_p , have been also calculated and tabulated in Table 4 using the formulas:

$$G_c = \frac{K_c^2}{E} \quad \dots (4)$$

$$\delta_c = \frac{G_c}{\sigma_0} \quad \dots (5)$$

Table 4. Fracture Characteristics Results

Aging Time hrs	Fracture Toughness Kc, MPa \sqrt{m}	Critical Energy Release Rate Gc, MPa. mm	Critical Crack opening Dis- placement δ_c , mm	Critical Plastic Zone size, r_p , mm
1/2	42.45	25.4	0.0508	7.208
2	48.25	32.8	0.0656	9.312
5	37.50	19.8	0.0396	5.625
10	25.10	8.9	0.0178	2.520

Fig.4 illustrates the variation of the fracture characteristics with aging time, while Fig.5 is a log-log plot of the same quantities.

As described above, the process of crack propagation under small scale yielding condition can be correlated with the nominal stress intensity range, ΔK , with the variation between da/dN and ΔK being sigmoidal in shape over a wide range of growth rates, as shown in Fig.1. The simple power law relationship, Eq. (1), provides a reasonable description of behavior in the intermediate range of growth rates between 10^{-6} and 10^{-3} mm/cycle. Deviations from such behavior take place at lower ΔK levels approaching the threshold values and at higher growth rates approaching instability and fracture. Since the majority of fatigue lifetime must be spent where the crack is growing most slowly, it generally is the near-threshold and intermediate regions which dominate life of the component.

Plots of the fatigue crack length versus number of cycles for all specimens are shown in Figures 6,7, and 8. These plots were used to determine the rate of crack growth (CGR), da/dN . The excursion in the stress intensity factor, ΔK , which corresponds with crack lengths, a , were calculated using the equation [6].

$$\Delta K = (\Delta\sigma)\sqrt{\pi a} f(a/b) \quad \dots (6)$$

where $\Delta\sigma$ is the excursion in the stress,
 $f(a/b)$ is a function given, for SEN specimens, as follows [6], Table 5 :

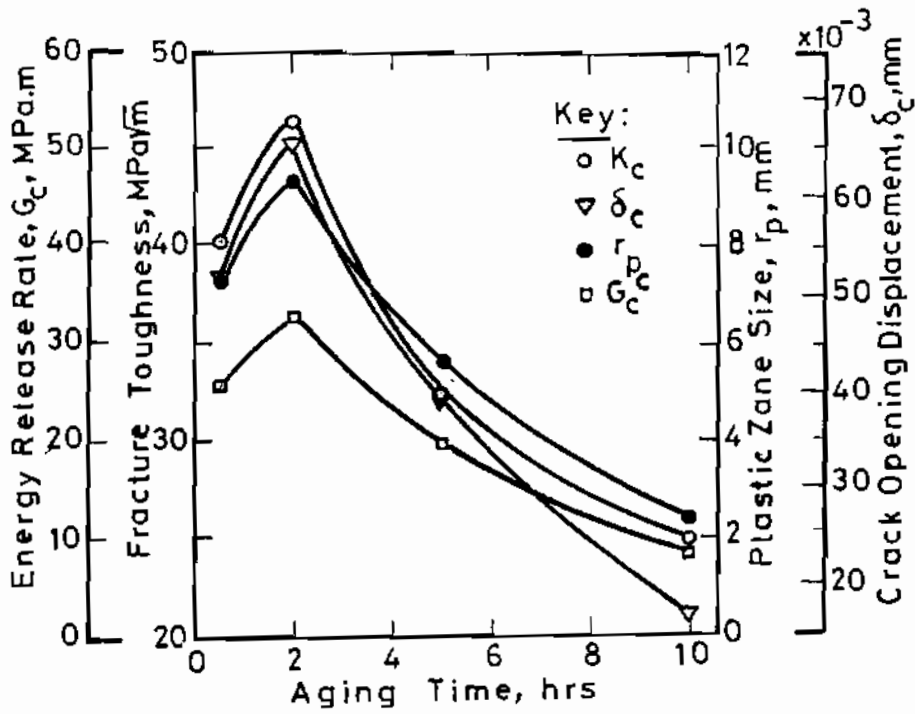


Fig.4 Variation of Fracture Characteristics with Aging Time

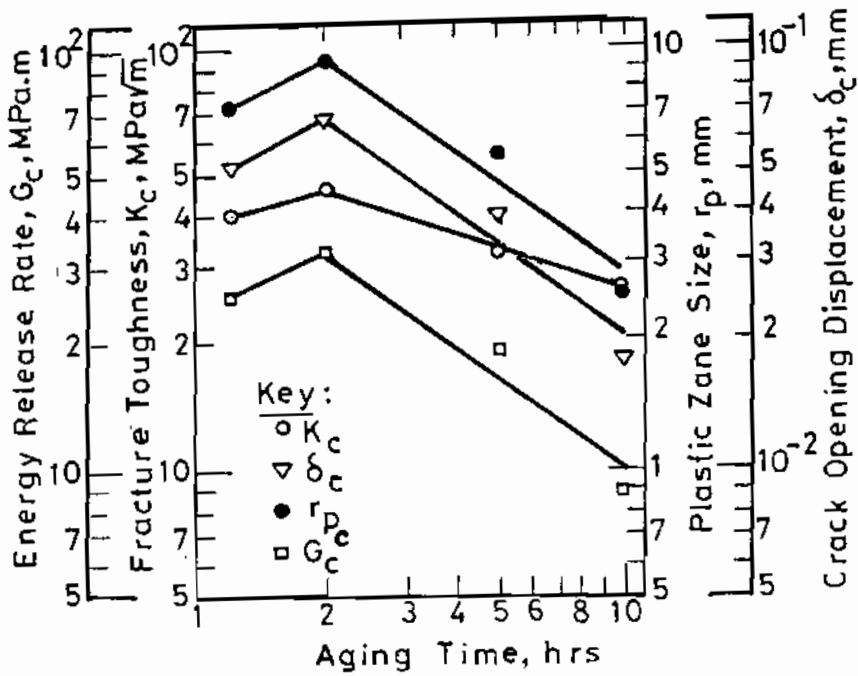


Fig.5 Variation of Fracture characteristics with Aging Time on a Logarithmic Scale

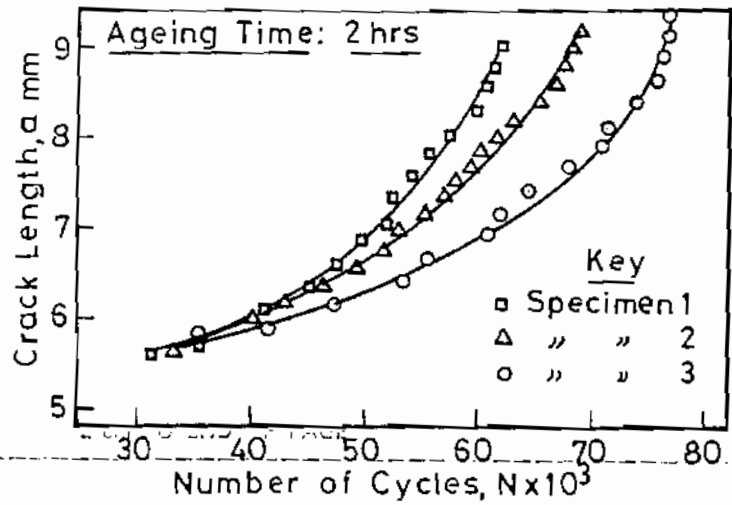


Fig.6 Crack Growth Curve For Aging Time of 2 hours

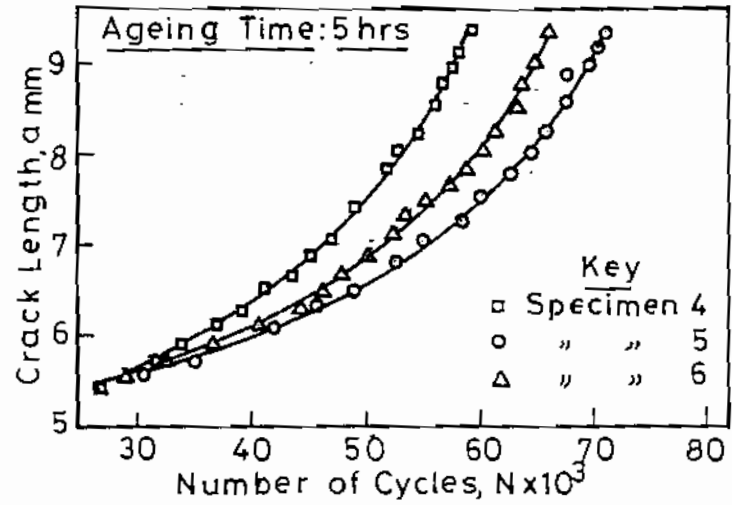


Fig.7 Crack Growth Curve for Aging time of 5 hours

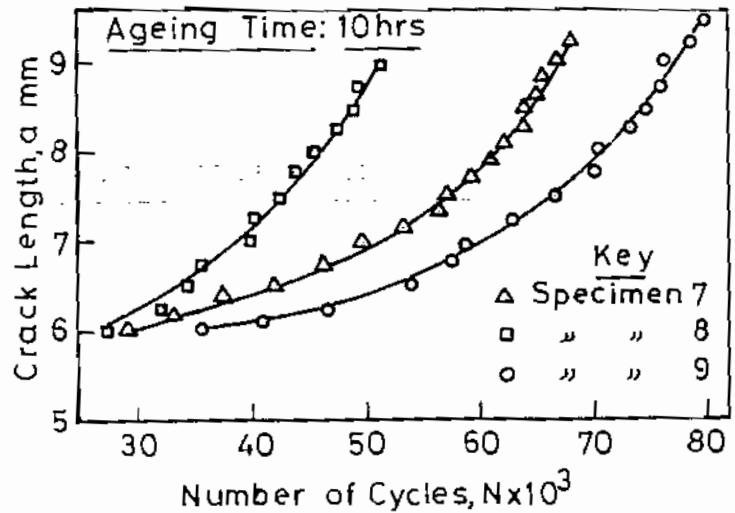


Fig.8 Crack Growth Curve for Aging Time of 10 hours

Table 5 function, $f(a/b)$, for SEN specimens

(a/b)	0.1	0.3	0.6	0.9
f(a/b)	1.14	1.24	1.66	2.44

Crack lengths in Eq. (3) have been corrected for plasticity effects [7] and the stress intensity factors and the fracture toughness were recalculated accordingly.

The resulting values of the crack growth rates, da/dN , which were calculated from Figs. 6,7, and 8, were plotted against the excursion in stress intensity factor, ΔK , on a log-log paper. Figs. 9,10 and 11 show the resulting straight line relationships, the intermediate sections of the sigmoidal curves, from which the parameters A and m were calculated. Table 6 and Fig. 12 give a summary of the test results.

Table 6 Summary of Test Results

Ageing Temp., °C	Ageing Time, hr	Average "A"	Average "m"
177	10	2.50×10^{-10}	4.30
177	5	9.95×10^{-10}	4.05
177	2	21.5×10^{-10}	3.60

Fig. 13 illustrates a log-log plot of the parameters A and m with the aging time.

DISCUSSION OF TEST RESULTS

The relationships exhibited in Fig.4 represent the plane stress fracture toughness, K_{IC} , the critical energy release rate, G_C , the critical crack opening displacement, δ_C , and the critical plastic zone size, r_{pC} , as influenced by the aging time, t_a . It is seen that these fracture characteristics increase with increasing the aging time for the under-aged material, i.e. the material with smaller aging time, reaching peak values at an aging time of two hours for the aging temperature of the test. For over-aged material, i.e. the material with longer aging period, the fracture characteristics reduce as the aging time increases.

Exponential regression analysis has been performed on the test results shown in Fig 4 [3]. The fracture characteristics, i.e. the plane stress fracture toughness, K_{IC} , the critical strain energy release rate, G_C , the critical crack opening displacement, δ_C , and the critical plastic zone size, r_{pC} , have been related to the aging time, t_a , through a set of exponential equations in the form.

$$Y_1 = A_1 e^{B_1 t_a} \quad (7)$$

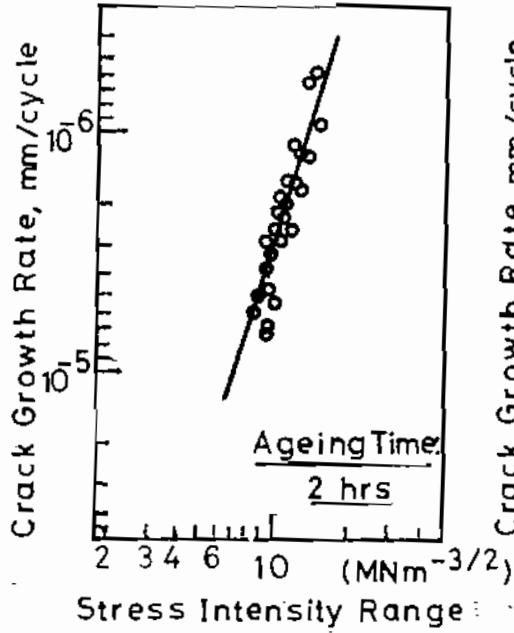


Fig.9 Logarithmic Crack Growth Curve (2 hours Aging)

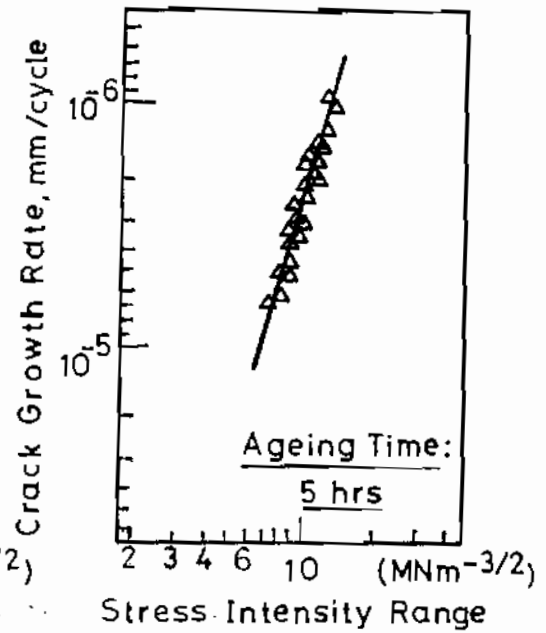


Fig.10 Logarithmic Crack Growth Curve (5 hours Aging)

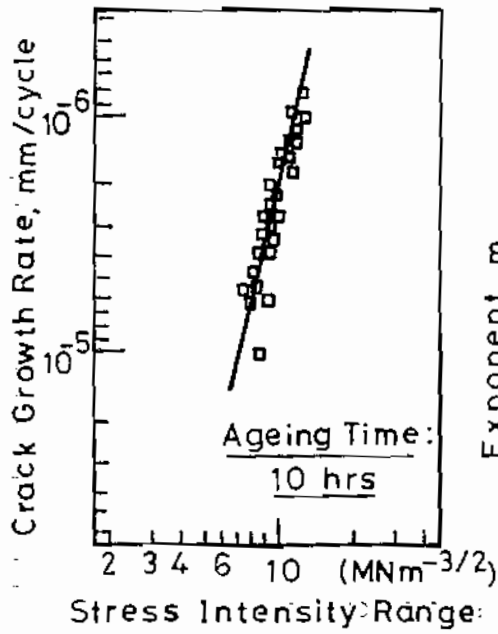


Fig.11 Logarithmic Crack Growth Curve (10 hours Aging)

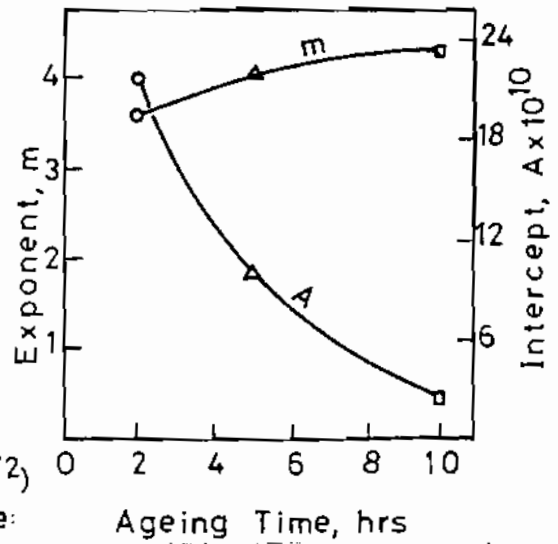


Fig.12 Crack Growth Law Parameters, A & m, with Aging Time

In Eq. (7), Y_i , where $i = 1,2,3,4$, represent the four fracture characteristics mentioned above, respectively. The coefficients A_i and B_i which have been determined from the regression process are listed in Table 7.

Table 7 Coefficients of the Exponential Regression Analysis

Regression Coefficients	for Plane Strain Fracture Toughness, K_c	for Critical Strain Energy Release Rate, G_c	for Critical Crack Opening Displacement, δ_c	for Critical Plastic Zone Size, r_{pc}
Coefficient A_i	49.16	34.64	6.81×10^{-2}	9.67
Coefficient B_i	-6.34×10^{-2}	-0.13	-0.13	-0.13
Coeff. of Determination	0.8811	0.8814	0.8814	0.8811
" Correlation	0.9387	0.9388	0.9388	0.9387
Standard Error of Estimation	0.1194	0.2381	0.2381	0.2388

The values of the parameters A & m , as shown in Fig. 12, reflect the type of crack propagation behavior of 7075-T6 aluminum alloy as a function of aging time. The two parameters, and hence the cracking behavior, are seen to be strongly dependent on the heat treatment performed on the material. The exponent m is shown to have a direct relationship with the ageing time, while the intercept A is having an inverse one. The parameter A for two hours aging time is about ten times its value for ten hours, while the increase in the magnitude of m is about 16%. The resulting conclusion is generally an increase in the crack propagation rate with longer aging periods, which seems to be in agreement with previous studies on other age-hardened materials [9].

The dependence of the parameters A and m of Paris equation, Eq. (1), on the aging time, t_a , may be represented in a mathematical form, based on Fig. 13, as follows:

$$A = A' t_a^{n1} \quad \& \quad m = m' t_a^{n2} \tag{8}$$

where $A', m', n1$ and $n2$ are a new set of parameters to be determined from the experimental data, as illustrated in Table 8.

Table 8 Experimental Values of Crack Growth Rate Parameters

A'	$n1$	m'	$n2$
6.3×10^{-9}	$-\frac{4}{3}$	3.1	$\frac{1}{7}$

It is well known that the rate of crack growth depends on the intensity of the stress and strain fields at the tip of the crack, i.e. the range of stress intensity factor, ΔK . The rate of crack growth is directly proportional to the range of stress intensity factor. In addition, the rate of crack growth is also dependent on the material properties and its resistance to initiation and growth.

Although the stress intensity factor range, ΔK , in the power law, Eq.1, is computed from geometry, crack size, and applied loading, the local driving force experienced at the crack tip may be different from the remote stress field. This may be due to various factors such as cyclic plasticity, crack path deviation, and crack closure; with the latter factor being most influential [10]. Crack closure occurring due to crack surface roughness, crack tip plasticity, and precipitates

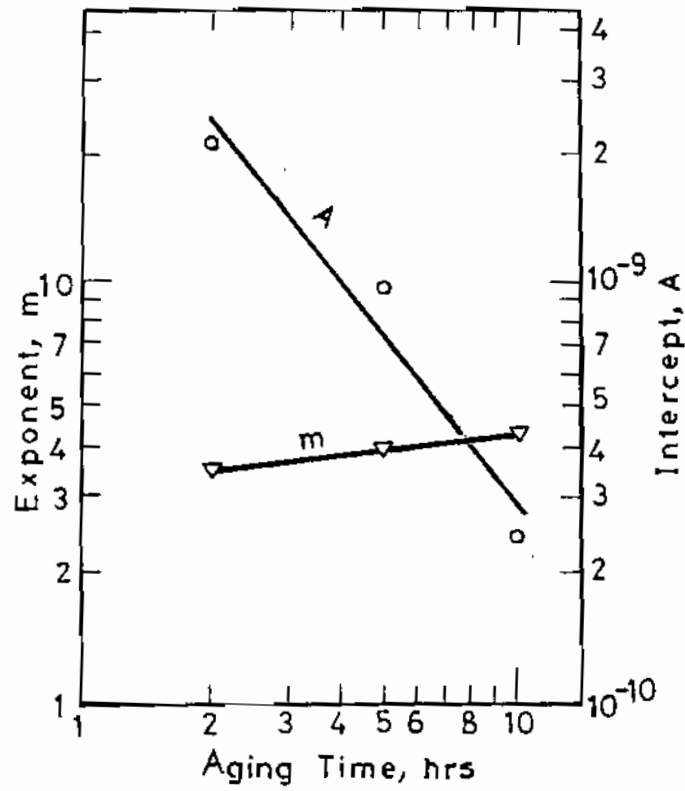


Fig.13 Crack Growth Law Parameters with Aging time on a log Scale

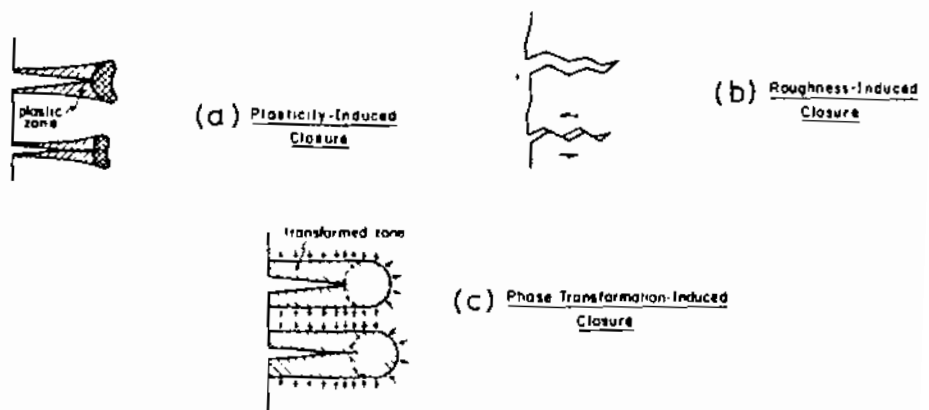


Fig.14 A Schematic Representation of Some Crack Closure Mechanisms.[10]

resulting from phase transformations, as illustrated in Fig.14, lead to an increase in the crack driving force and in crack propagation rate [10].

On the other hand, crack path deviation has been proven to occur on both microstructural and macrostructural scales in aluminum alloys and steel [9,11,12]. The cause of the deviation of crack growth direction is attributed to the material's microstructure and the applied stress state being uniaxial or multiaxial. It has been shown that in all cases of crack path deviation, the rate of fatigue crack growth tends to decrease or stay constant at the value at the onset of turning [9,11]. Figs. 15 & 16 illustrate the crack path deviation [9, 11, 12].

As to the aluminum alloy tested in this study, it was observed that the fracture characteristics and the fatigue crack growth are affected by the aging time. As the aging time increases, the fracture resistance of the material decreases while the rate of fatigue crack growth increases. Ritchie and Thompson [13] estimated the rate of energy release at the onset of instability, J_{ss} , as being a function of the material's strength, σ_0 , the ductility, ϵ_0 , and the interparticle spacing, l_0 , as follows:

$$J_{ss} = (\sigma_0^2/E) l_0 \exp \left[\frac{0.6(1+\nu)}{(2-\nu)} \frac{\epsilon_f}{\epsilon_0} \right] \quad \dots (9)$$

From Eq.9, the critical rate of energy release, and all other fracture characteristics, increase with increasing the ductility, decreasing strength, and increasing the interparticle spacing. In all age-hardening aluminum alloys, the process of diffusion and accumulation of second phase particles increase as the aging time increases. As a result of this process, there will be an increase in the local strain in the material which causes hindering of the motion of dislocation. This will lead to increasing the strength and decreasing the ductility which results in reducing the fracture toughness and other fracture characteristics [14,15].

The explanation for the variation of the rate of fatigue crack growth with aging time may be based on the hardening scheme which occurs in the microstructure [10]. Underaged microstructures are hardened primarily by the shearing of small coherent precipitates resulting in planar slip systems which promotes crystallographic crack paths. The increased resistance to crack growth will, therefore, be the result of an increase in crack closure in addition to crack tendency to deviate from its principal direction. The result will be slower crack growth rate.

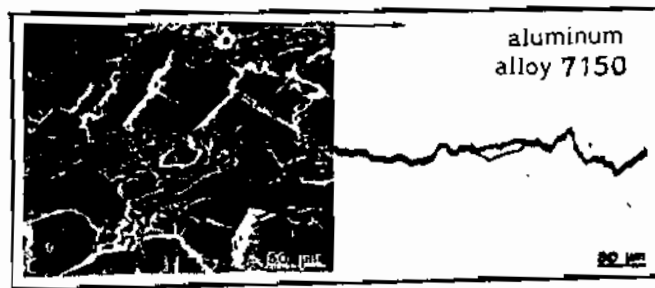
On the other hand, in overaged microstructures, the mode of hardening is one of Orowan bypassing around larger non-shearable precipitates. The resulting wavy slip system which consists of a large number of finer slip steps, generates planar fracture surfaces. This leads to less roughness-induced closure resulting in more crack extension per cycle [10,16].

CONCLUSIONS

In this study, an attempt has been made to highlight the fatigue crack growth and fracture characteristics of Cu-Mg-Zn aluminum alloy (7075) and their variation with the aging time.

The following conclusions may be made:

- (1) The fracture toughness, K_{IC} , the critical strain energy release rate, G_C , the critical crack opening displacement, δ_C , and the critical plastic zone size, r_{pC} , all increase with aging time for underaged alloy and then decrease after reaching peak values at a certain aging time. This is explained as being the result of the resistance to the dislocation motion due to the diffusion of the second phase precipitates.



(a)

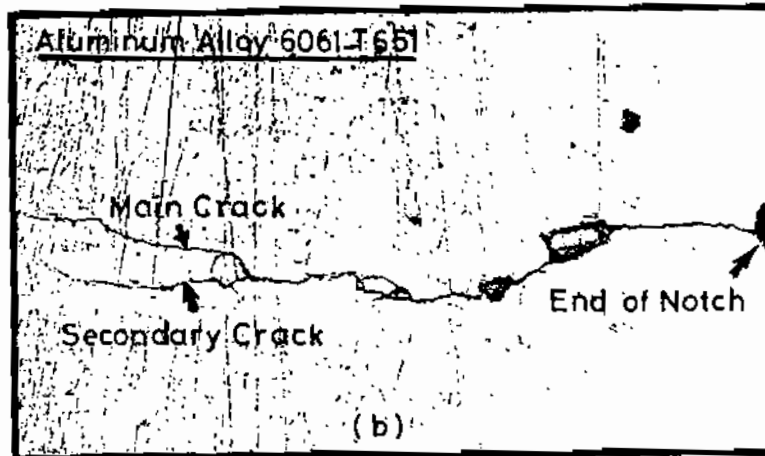


Fig.15 Crack Growth Pattern in Aluminum Alloys [9,11]

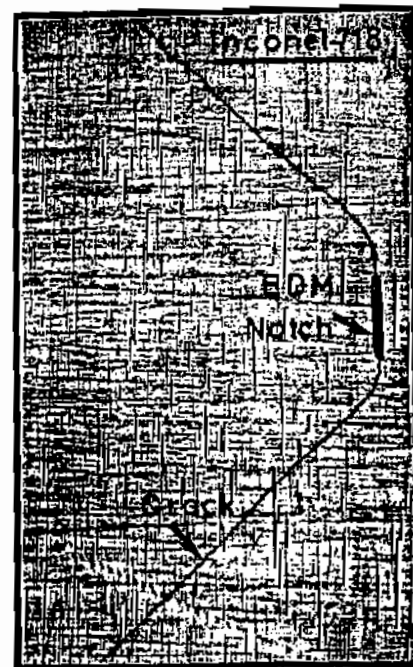
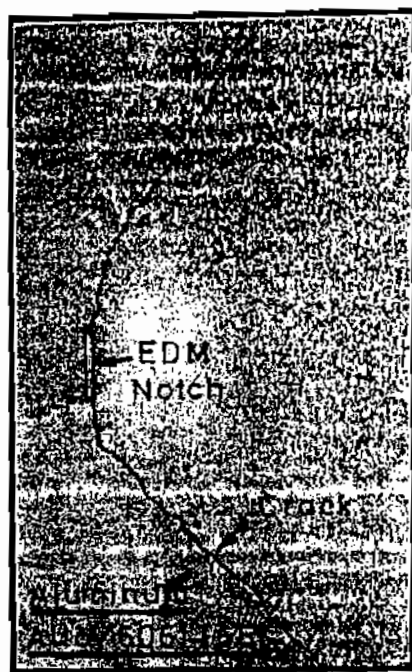


Fig.16 Crack Path Deviation Under Biaxial Stress Fields in an Aluminum Alloy and Inconel 718 [9,11,12]

- (2) The rate of fatigue crack growth was observed to be low for underaged alloy and increased with aging time. This is explained as being due to the slip system and the hardening scheme which occurs in the microstructure due to aging.

REFERENCES

1. Paris, P.C. and Erdogan, F., "A Critical Analysis of Crack Propagation Laws," ASME Trans., J. Basic Engg., Series D, 1963
2. Lai, Z.H. and Ma, C.X., "Comparison of Several Methods of J_{IC} Determination," Eng. Fract. Mech., Vol. 22, No. 6, 1985
3. Matsoukas, G., Cottrell, B. and Mai, Y.W., "The Effect of Geometry on the Crack Opening Displacement of a Low Carbon Steel," Engineering Frac. Mechanics, Vol. 23, No. 4, 1986
4. Chow, C. L., Woo, C. W. and Chung, K. T., "Fatigue Crack Propagation in Mild Steel," Eng. Frac. Mech., Vol 24 NO. 2, 1986
5. Shiozawa, K., Asamoto, T. and Miyao, K., "Crack Propagation Behavior Under Low-Cycle Corrosion Fatigue of A7003-T6 Aluminum Alloy," Jap. Soc. Mech. Eng. (JSME) Int. Journal, Series 1, Vol. 32, No. 4, 1989
6. Feddersen, C.E., Simonen, F.A., Huinert, L.E., and Hylder, W. S., "An experimental and Theoretical Investigation of Plane Stress Fracture of 2024-T351 Aluminum Alloy," "NASA-CR-1678, 1970
7. Rice, J. R., "Mechanics of Crack Tip Deformation and Extension by Fatigue," "ASTM-STP 415, American Soc. for Testing Materials, 1967
8. Science and Engineering Programs Apple II Edition, Edited by John Heilborn, Osborne-Mc Grae Hill, Berkeley, California, U.S.A.
9. Zaiken, E. and Ritchie, R.O., Material Science Eng., 68, 1984
10. Ritchie, R.O., "Slow Crack Growth: Macroscopic and Microscopic Aspects," "Fracture & Fracture Mechanics, Case Studies, Proc. of Second National Conf. Conf. on Fracture, Johannesburg, S.Africa, 1984
11. Zamrik, S.Y. and Shabara, M.A., "The Effect of Stress Ratio on Fatigue crack Growth in a Biaxial Stress Field," "Trans. of the ASME, J. of pressure Vessel Technology, Paper No. 76-PVP-37, Feb. 1977
12. Shabara, M.A.N., "A Method for the Prediction of Crack Growth Direction in a Biaxial Stress Field," Proc. of the Int. AMSE Conf. on Modelling & Simulation, Paris, France, Vol. 7, 1982
13. Ritchie, R.O. and Thompson, A.W., Metall. Trans., 15A, 1984
14. Unwin, P.N.T. and Smith, G.C., "The Microstructure and Mechanical Properties of Al-6% Zn-3% Mg," J. Inst. Met. 91, 1969
15. Shabara, M.A.N., "Correlations of Fracture Toughness to the Strength and Ductility of Aluminum Alloys," First Conf. for Theoretical & Applied Mechanics, Cairo, Dec. 1980
16. Shabara, H.A.N., and Fattah, A.A., "Fatigue Crack Initiation and Growth in High-Strength Aluminum Alloy," Proc. Inter. AMSE Conf. on "Modelling & Simulation," Istanbul, Turkey, 1988, AMSE Press, Vol. 3A